Symposium on Fundamental Issues in
Elementary Matter (2000) 000–000

Fundamental Issues in Elementary Matter
Bad Honnef, Germany
September 25–29, 2000

Hydrodynamic Models for Heavy-Ion Collisions, and beyond

A. Dumitru[1,a], J. Brachmann[2], E.S. Fraga[3], W. Greiner[2], A.D. Jackson[4], J.T. Lenaghan[4], O. Scavenius[4], H. Stöcker[2]

[1] Physics Dept., Columbia Univ., 538 W. 120th Street, New York, NY 10027, USA
[2] Institut für Theor. Physik, J.W. Goethe Univ., Robert-Mayer Str. 10, 60054 Frankfurt, Germany
[3] Brookhaven National Laboratory, Upton, NY 11973, USA
[4] The Niels Bohr Institute, Blegdamsvej 17, DK-2100 Copenhagen Ø, Denmark

Abstract. A generic property of a first-order phase transition *in equilibrium*, and in the limit of large entropy per unit of conserved charge, is the smallness of the isentropic speed of sound in the "mixed phase". A specific prediction is that this should lead to a non-isotropic momentum distribution of nucleons in the reaction plane (for energies $\sim 40A$ GeV in our model calculation). On the other hand, we show that from present effective theories for low-energy QCD one does not expect the thermal transition rate between various states of the effective potential to be much larger than the expansion rate, questioning the applicability of the idealized Maxwell/Gibbs construction. Experimental data could soon provide essential information on the dynamics of the phase transition.

1. Introduction

Heavy-ion collisions at high energy are devoted mainly to the study of strongly interacting matter at high temperature and density. In particular, a major focus is the search for observables related to restoration of chiral symmetry and deconfinement, as predicted by lattice QCD to occur at high temperature, and in thermodynamical equilibrium [1]. Also, various effective models for low-energy QCD predict chiral symmetry restoration at high net baryon density and low temperature [2].

Several observables for the transition to deconfined matter have been proposed, such as electromagnetic radiation, strangeness enhancement and equilibration, charmonium dissociation, and "irregularities" in the hydrodynamic flow pattern [3]. The latter, in particular, represents an observable that is related to the effective potential at finite temperature and density, because hydrodynamical expansion is driven by pressure gradients, and the pres-

xxxxx-xxx/2000

sure is minus the value of the effective potential at the global minimum. Therefore, if indeed a new minimum of the effective potential opens up at some temperature or density, the pressure gradients should change and allow observation of that new state. Here, we discuss the differential distribution of the momenta of nucleons in the reaction plane (spanned by the beam axis and the impact parameter axis) as an observable for the emergence of a second minimum of the effective potential, which defines a new thermodynamical state of hot matter. Finally, we shall discuss if a phase transition close to equilibrium is likely to be a reasonable approximation, how one can improve on that model, and possible consequences for observables.

2. Effective Potential for the Chiral Phase Transition

For illustration, consider the following Lagrangian for the approximately $O(4)$ symmetric chiral field $\Phi = (\sigma, \pi)$ coupled to (constituent) quarks $q = (u, d)$:

$$\mathcal{L} = \overline{q}[i\gamma^\mu \partial_\mu - g(\sigma + i\gamma_5 \tau \cdot \pi)]q + \frac{1}{2}(\partial_\mu \sigma \partial^\mu \sigma + \partial_\mu \pi \partial^\mu \pi) - U(\sigma, \pi) \quad . \tag{1}$$

The potential, exhibiting both spontaneously and explicitly broken chiral symmetry, is

$$U(\sigma, \pi) = \frac{\lambda^2}{4}(\sigma^2 + \pi^2 - v^2)^2 - H_q \sigma \quad . \tag{2}$$

The vacuum expectation values of the condensates are $\langle \sigma \rangle = f_\pi$ and $\langle \pi \rangle = 0$, where $f_\pi = 93$ MeV is the pion decay constant. The explicit symmetry breaking term is due to the finite current-quark masses and is determined by the PCAC relation which gives $H_q = f_\pi m_\pi^2$, where $m_\pi = 138$ MeV is the pion mass. This leads to $v^2 = f_\pi^2 - m_\pi^2/\lambda^2$. The value of $\lambda^2 = 20$ (used throughout this paper) leads to a σ-mass, $m_\sigma^2 = 2\lambda^2 f_\pi^2 + m_\pi^2$, equal to 600 MeV. For $g > 0$, the finite-temperature one-loop effective potential also includes the following contribution from the quarks:

$$V_q(\Phi) = d_q T \int \frac{\mathrm{d}^3 k}{(2\pi)^3} \log\left(1 + e^{-E/T}\right) \quad . \tag{3}$$

Here, $d_q = 24$ denotes the color-spin-isospin-baryon charge degeneracy of the quarks. $V_q(\Phi)$ depends on the order parameter field Φ through the effective mass of the quarks entering the expression for the energy $E \equiv \sqrt{k^2 + g^2\Phi^2}$. The quarks constitute the heat bath in which the long-wavelength modes of the chiral field, i.e. the order parameter, evolve, resulting in the finite-temperature effective potential $V_{\rm eff} \equiv U + V_q$. For rather large values of g, the theory exhibits a first-order (chiral symmetry restoring) phase transition. For example, for $g = 5.5$ the critical temperature is $T_c = 123.7$ MeV at vanishing baryon-chemical potential μ. At the phase transition line in the $T - \mu$ plane, $V_{\rm eff}$ exhibits two degenerate minima labeled (a) and (b) in Fig. 1, respectively. The first is the thermodynamical state corresponding to restored chiral symmetry, while the second corresponds to broken symmetry and smoothly approaches the physical vacuum at $T = 0$. The two states are separated

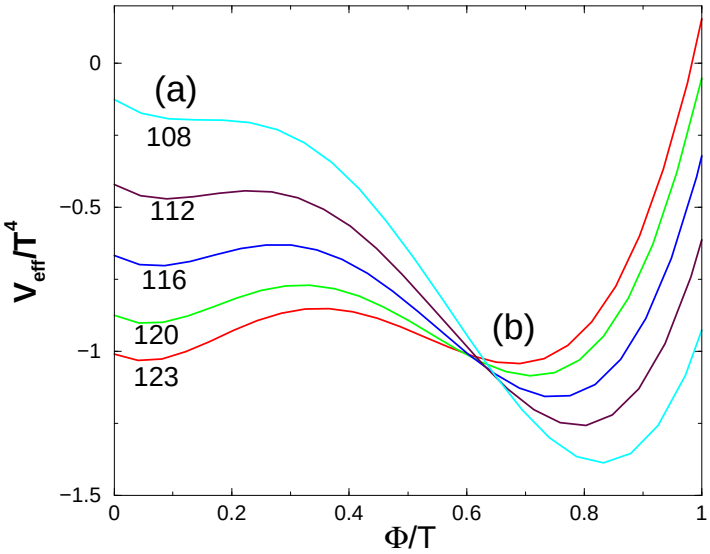

Fig. 1. An example for a finite-temperature effective potential exhibiting two states (a) and (b), respectively, as a function of the order parameter field Φ in σ-direction and temperature T, for vanishing net baryon charge. See text and ref. [4] for details.

by a barrier which becomes smaller as the temperature decreases, ending in a point of inflection at $T_{sp} \approx 108$ MeV (for our set of parameters and $\mu = 0$), the so-called spinodal instability. At this temperature, there is no more barrier to the true ground state and the order parameter "rolls" down towards the state (b), a process called spinodal decomposition. In thermodynamical equilibrium, the order parameter is localized in either one of the two minima, whichever is at lower energy. At the phase boundary, where the two states are degenerate, the system is in the "mixed phase", the expectation value of Φ being peaked both about $\Phi_{(a)}$ as well as $\Phi_{(b)}$. A Maxwell construction can be performed two obtain the relative probabilities for the system to be in either of the two states.

If one is interested in the hydrodynamical evolution of a system in local equilibrium, and described by the effective potential $V_{\rm eff}$, all one needs to know is the value of $V_{\rm eff}$ at its global minimum, which is the value of the grand canonical potential (density) at the given temperature and chemical potential, i.e. minus the pressure. Once the function $p(T,\mu)$ is known, the evolution (in local equilibrium) of some initial condition is uniquely determined by the equations of ideal relativistic hydrodynamics.

3. Hydrodynamics of Strongly Interacting Matter

Hydrodynamics is defined by (local) energy-momentum and net charge conservation [5],

$$\partial_\mu T^{\mu\nu} = 0 \quad , \quad \partial_\mu N_i^\mu = 0 \quad . \tag{4}$$

$T^{\mu\nu}$ denotes the energy-momentum tensor, and N_i^μ the net four-current of the ith conserved charge. We will explicitly consider only one such conserved charge, namely the net baryon number. We implicitly assume that all other charges which are conserved on strong-interaction time scales vanish locally. The corresponding four-currents are therefore identically zero, cf. eq. (5), and the conservation equations are trivial.

For ideal fluids, the energy-momentum tensor and the net baryon current assume the simple form [5]

$$T^{\mu\nu} = (\varepsilon + p)\, u^\mu u^\nu - p g^{\mu\nu} \quad , \quad N_B^\mu = \rho u^\mu \quad , \tag{5}$$

where ε, p, ρ are energy density, pressure, and net baryon density in the local rest frame of the fluid, which is defined by $N_B^\mu = (\rho, \mathbf{0})$. $g^{\mu\nu} = \mathrm{diag}(+,-,-,-)$ is the metric tensor, and $u^\mu = \gamma(1,\mathbf{v})$ the four-velocity of the fluid ($\mathbf{v}$ is the three-velocity and $\gamma = (1-\mathbf{v}^2)^{-1/2}$ the Lorentz factor). The system of partial differential equations (4) is closed by choosing an equation of state (EoS) in the form $p = p(\varepsilon, \rho)$.

The EoS employed in this section exhibits a first order phase transition to a Quark-Gluon Plasma (QGP). The hadronic phase consists of nucleons interacting via relativistic scalar and vector fields [6]; the pressure is obtained from the one-loop effective potential for the nucleons, similar to eq. (3), plus that of free thermal pions. The QGP phase is described within the framework of the MIT-Bag model as an ideal gas of u and d quarks and gluons, with a bag parameter $B^{1/4} = 235$ MeV, resulting in a critical temperature $T_c \simeq 170$ MeV at $\rho = 0$, while the critical baryon-chemical potential is $\mu_c = 1.8$ GeV at $T = 0$. The first order phase transition is constructed via Gibbs' conditions of phase equilibrium. Thus, by construction the two states of the effective potential are coexisting in equilibrium: as the fluid expands, an increasing fraction of matter is transfered from the high-temperature state (a) to the low-temperature state (b). Supposedly, that happens through nucleation of bubbles of hadronic matter within the QGP matter [7, 4]. If that process occurs arbitrarily close to equilibrium, the two thermodynamical states remain degenerate throughout the phase transition region, such that the pressure is the same in both states.

3.1. The effect of a first-order equilibrium phase transition on directed flow

The equilibrium (first-order) transition discussed above has interesting implications regarding the hydrodynamical expansion pattern of the hot and dense matter [8]. Expansion of a perfect fluid conserves the entropy current $s^\mu = s u^\mu$, as follows from eqs. (4) upon contraction with the contravariant four-velocity u_ν, and from the thermodynamical identities $\mathrm{d}\varepsilon = T\,\mathrm{d}s + \mu\,\mathrm{d}\rho$, $\varepsilon = Ts - p + \mu\rho$. Thus, the entropy density current s^μ is proportional to the baryon density current N_B^μ; each fluid element traces a path of $s/\rho = \text{const.}$ in the phase diagram. The pressure gradient among neighbouring fluid elements, which is responsible for the acceleration in a given spatial direction, is given by $\nabla p = c_s^2 \nabla\varepsilon$, where

$$c_s^2 \equiv \left.\frac{\partial p}{\partial \varepsilon}\right|_{s/\rho=\text{const.}} \tag{6}$$

denotes the isentropic speed of sound. Fig. 2 shows the pressure as a function of the energy

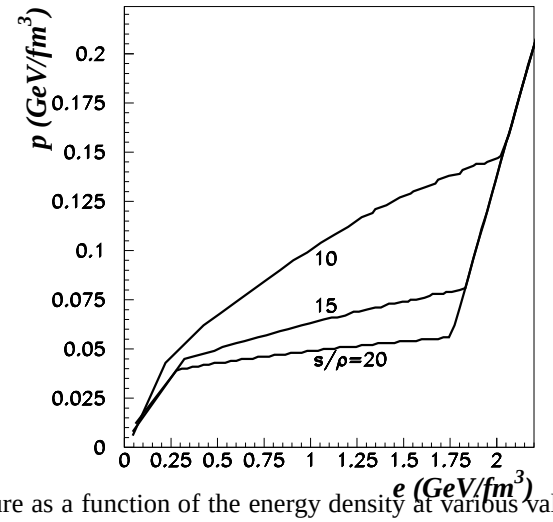

Fig. 2. The pressure as a function of the energy density at various values for the specific entropy (for the EoS described in the text).

density at various values for the specific entropy s/ρ. (The "wiggles" in the curves are due to the plotting procedure and do not reflect the numerical accuracy, which is much better.) One clearly observes a rapid increase of $p(\varepsilon)$ within the hadronic phase, followed by a less rapid increase in the coexistence ("mixed") phase, and finally the transition to pure quark-gluon matter at very high energy density. In particular, the hotter the fluid, that is the larger s/ρ, the more does $p(\varepsilon)$ flatten out in the mixed phase. For $s/\rho \to \infty$ we obtain $p = \text{const.}$ inbetween the two pure phases. That behavior can be understood immediately as following from Gibbs' conditions of phase equilibrium. $s/\rho \to \infty$ implies $\mu/T \to 0$, and thus in this limit the temperature is the only remaining intensive thermodynamical variable the effective potential (and the pressure) can depend on. Now, in phase equilibrium $T = T_c = \text{const.}$ and so the pressure $p(T_c) \equiv p_c$ is constant as well. In other words, the isentropic speed of sound c_s^2 must be small during the time when a fluid element's trajectory through the phase diagram coincides with the phase coexistence line (in the $T-\mu$ plane).

If that prediction based on the equilibrium phase diagram is indeed relevant for collisions of heavy ions, it should be visible in the excitation function of the so-called directed in-plane flow [8, 9], $\langle p_x/N \rangle$. That observable is defined as the average momentum per nucleon in impact parameter ($x-$) direction [10], and due to the kinematics of the collision is particularly sensitive to the early stage of the reaction, where the phase transition might occur. A more refined observable is the distribution of momentum in the reaction plane, which is proportional to the triple-differential cross section for the process $AB \to p + X$, $\mathrm{d}\sigma/\mathrm{d}^3 p$. To zeroth approximation, it can be obtained by integrating the baryon current N_B^μ over the freeze-out hypersurface of the nucleons, Σ^μ:

$$\frac{\mathrm{d}\sigma}{\mathrm{d}^3 p} \propto \int \mathrm{d}\Sigma_\mu N_B^\mu \delta(m_N \mathbf{u} - \mathbf{p}) \quad . \tag{7}$$

In what follows we assumed for simplicity that freeze-out, or at least onset of strong dis-

sipative correction to the perfect-fluid energy-momentum tensor, occurs on an equal-time hypersurface in the center of mass frame, $d\Sigma^\mu = (d^3x, \mathbf{0})$. Furthermore, we integrated the differential cross section over the momentum component p_y, perpendicular to both the impact parameter vector and the beam axis.

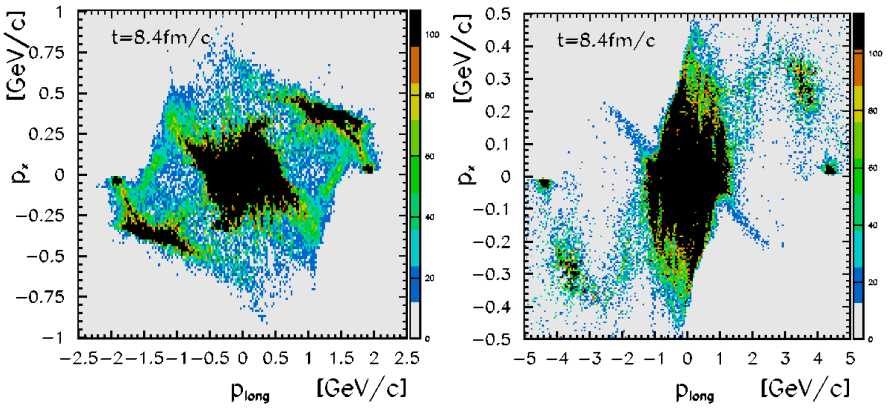

Fig. 3. Distribution of the time-like component of the net-baryon four-current in momentum space ($p_x - p_z$ plane). Pb+Pb collisions at $b = 3$ fm, $E^{kin}_{Lab} = 8A$ GeV (left frame) and $40A$ GeV (right frame), respectively.

Typical distributions of nucleons in momentum space are depicted in Fig. 3 [11]. The left frame corresponds to relatively low collision energy and specific entropy $s/\rho \approx 10$. Therefore, c_s^2 is not small in that case even if the energy density at the center exceeds ~ 0.5 GeV/fm^3, and the state (a) of the effective potential should be populated according to the equilibrium EoS (see Fig 2). So, since c_s^2 is not small, (energy-) density gradients in coordinate space reflect in non-vanishing pressure gradients ∇p, which in turn act to make the distribution of nucleons in momentum space more or less isotropic. The *net* momentum in x-direction at any fixed longitudinal momentum p_z is obviously rather small, as positive and negative contributions largely cancel [12].

On the other hand, Fig. 3 also shows that the structure of the flow changes qualitatively at higher energy, $E^{kin}_{Lab} \approx 40A$ GeV, where on average $s/\rho \approx 20$. The fact that c_s^2 is now smaller than at lower energy, by a factor of two in the present model, actually *prevents* more isotropic redistribution of the baryon number in momentum-space [11]. The distribution is clearly very different from that at the lower energy, with almost no nucleons in the upper left or bottom right quadrants where $p_x \cdot p_z < 0$ [11].

4. The nucleation rate, and supercooling down to the spinodal

The Gibbs/Maxwell construction relies on the assumption that the thermal barrier penetration rate is much larger than the local expansion rate. In a slowly expanding system, the phase transition would proceed through the nucleation of bubbles of the "true vacuum" state via thermal activation [7, 4]. The nucleation rate per unit volume per unit time is

expressed as

$$\Gamma = \mathcal{P}\ e^{-F_b/T} \quad , \tag{8}$$

where F_b is the free energy of a critical bubble and where the prefactor $\mathcal{P}$ provides a measure of the saddle point of the Euclidean action in functional space. Our analysis will concentrate on the exponential barrier penetration factor, and we will approximate $\mathcal{P}$ by T^4, which is obtained from dimensional considerations at $\mu = 0$. In order to determine the role of bubble nucleation in the evolving system and to be able to compute the decay rate Γ, it is necessary to study the critical bubble and some of its features. The critical bubble is a radially symmetric, static solution of the Euler-Lagrange field equations that satisfies the boundary condition $\Phi(r \to \infty) \longrightarrow \Phi_{(a)}$. Energetically, this boundary condition corresponds to an exact balance between volume and surface contributions which defines the critical radius $R = R_c$. The critical bubble is unstable with respect to small changes of its radius. For $R < R_c$, the surface energy dominates, and the bubble shrinks into the false vacuum. For $R > R_c$, the volume energy dominates, and the bubble grows driving the decay process.

The critical bubble can be found by minimizing the free energy

$$F_b(\Phi, T) = 4\pi \int r^2 \, \mathrm{d}r \left[\frac{1}{2} \left(\frac{\mathrm{d}\Phi}{\mathrm{d}r} \right)^2 + V_{\mathrm{eff}}(\Phi, T) \right] \quad , \tag{9}$$

with respect to the field Φ. This can be performed numerically without further approximation [4]. Fig. 4 shows the resulting decay rate, divided by an assumed expansion rate of

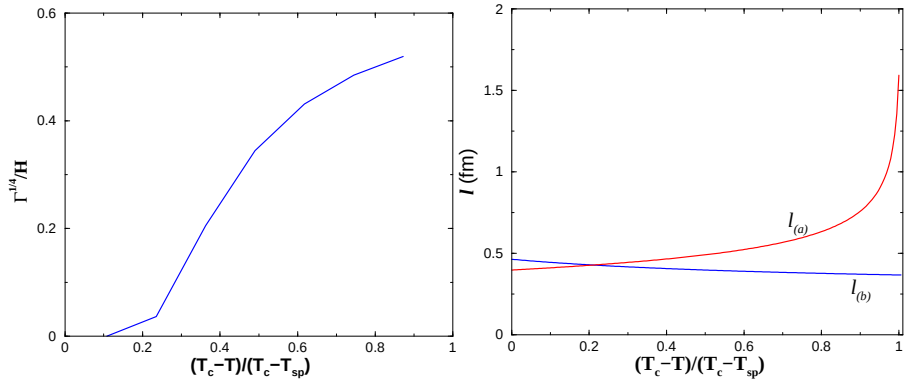

Fig. 4. $\Gamma^{1/4}$ divided by an assumed expansion rate of $H = 1$ fm^{-1} as a function of temperature (left frame). Correlation length of the chiral order parameter in state (a) and in state (b). The latter corresponds to an equilibrium transition.

$H = 1$ fm^{-1}, which represents a rough estimate for the expansion rate of the three-volume of a comoving fluid element, $\mathrm{d}V \equiv \mathrm{d}\Sigma \cdot u$, in high-energy collisions. $\Gamma^{1/4}$ specifies the inverse spatial and temporal scale of thermal field fluctuations into the broken symmetry state. Clearly, for the above effective field theory $\Gamma^{1/4}$ is not much larger than H, even if one takes into account that both factors are only known approximately. While the results of

Fig. 4 do not provide an unambiguous prediction for the fate of the supercooled state, they do make it appear likely that the rapidly expanding system has an appreciable probability of remaining in the restored symmetry phase even close to the spinodal instability. Thus, at least some fraction of all heavy ion events should show traces of this non-equilibrium transition. The familiar idealized Gibbs/Maxwell construction of equilibrium thermodynamics may not be appropriate for the description of phase transitions in high-energy heavy ion collisions. If so, the anisotropy of the differential nucleon cross section in the reaction plane, predicted in the previous section on the basis of the equilibrium phase diagram, should be *absent*. Rather, the small net momentum in impact parameter direction (around $p_z \sim 0$), as observed experimentally [13] at the top BNL-AGS energy $E_{Lab}^{kin} \approx 10A$ GeV, should remain essentially zero or diminish even further. That is because the phase equilibrium with small velocity of sound c_s^2 does not occur in a rapid out of equilibrium transition, where the order parameter remains localized in state (a) of the effective potential down to the spinodal.

Instead, other experimental observables of the phase transition may emerge. Consider the behavior of the correlation length of the Φ-field. It is obvious from Fig. 1 that the curvatures of the effective potential at the minima $\Phi_{(a)}$ and $\Phi_{(b)}$ are rather different for $T < T_c$. Thus, the effective mass, $m_{\rm eff}^2 = {\rm d}^2 V_{\rm eff}/{\rm d}\Phi^2$, and the correlation length, $l = 1/m_{\rm eff}$, of the field will also be different. In particular, if the rapidly expanding system supercools appreciably and if the order parameter is trapped in the metastable state, one can expect a clear increase of l. The right frame of Fig. 4 shows l in the states (a) and (b), respectively, as a function of the degree of supercooling. The correlation length at (a) increases as that minimum disappears. By contrast, there is a smooth decrease in the correlation length at the true global minimum, corresponding to an equilibrium transition. In the present model $l_{(a)}$ can exceed $l_{(b)}$ by as much as a factor of $2-3$, depending on the degree of supercooling. The precise values of l depend on the specific effective model adopted, but the qualitative observation that $l_{(a)}$ increases as the system approaches the spinodal instability is general.

5. Conclusions

We discussed generic properties of the effective potential for a first-order phase transition in equilibrium, in particular the vanishing of the isentropic velocity of sound in the limit of very large entropy per unit of conserved charge (baryon charge in our case). As an example for how such properties of the effective potential show up in the dynamics of hot and dense QCD matter we discussed the so-called directed flow of nucleons, i.e. the differential cross section in the reaction plane. Furthermore, we showed that the forthcoming results of the Pb+Pb reactions at $E_{Lab}^{kin} = 40A$ GeV can test the applicability of the picture of hot QCD-matter as a heat-bath with small isentropic speed of sound (mixed phase) to heavy-ion collisions in that energy domain. *If* it holds true, our model calculations predict an increase of the directed net in-plane momentum as compared to top BNL-AGS energy, and a nonisotropic momentum distribution around midrapidity. During the assumed first-order equilibrium phase transition pressure gradients along isentropes are too small to work towards a more isotropic momentum distribution.

The experimental test of the equilibrium phase transition picture would also provide

valuable constraints on effective field theories for low-energy QCD. As mentioned above, for the present model thermal barrier penetration from state (a) to state (b), and vice versa, is not materially larger than rough estimates for the expected expansion rates, thus leading to the possibility of significant supercooling, close to the spinodal instability.

The experimental observation of supercooling effects and spinodal decomposition would also be important as a matter of principle. Ideally, signatures of phase transitions should be order parameter related and should reveal properties of the equilibrium phase diagram. While the spinodal instability is not part of the equilibrium phase diagram, it is rather close. Familiar experiments in condensed matter physics on a wealth of hysteresis phenomena (i.e. the analogue of superheating and supercooling) make it clear that spinodal instabilities can be studied on "macroscopic" time scales [14]. The spinodal instability, if found, would certainly be among the most direct information which relativistic heavy ion collisions can provide regarding the QCD phase transition.

Acknowledgements

A.D. thanks the organizers for the invitation to attend and present this work, and also acknowledges support from DOE grant, Contract No. DE-FG-02-93ER-40764. E.S.F. is partially supported by the U.S. Department of Energy under Contract No. DE-AC02-98CH10886 and by CNPq (Brazil) through a post-doctoral fellowship. J.B. W.G. and H.S. acknowledge partial support by BMBF, DFG, and GSI.

Notes

a. E-mail: dumitru@nt3.phys.columbia.edu

References

1. F.R. Brown, N.H. Christ, Y.F. Deng, M.S. Gao, and T.J. Woch, Phys. Rev. Lett. **61** (1988) 2058; M. Oevers, F. Karsch, E. Laermann, and P. Schmidt, Nucl. Phys. Proc. Suppl. **63** (1998) 394; *ibid.* **73** (1999) 465.
2. I. Mishustin, J. Bondorf and M. Rho, Nucl. Phys. **A555** (1993) 215; P. Papazoglou et al, Phys. Rev. **C55** (1997) 1499; M.A. Halasz, A.D. Jackson, R.E. Shrock, M.A. Stephanov and J.J. Verbaarschot, Phys. Rev. **D58** (1998) 096007; M. Stephanov, K. Rajagopal and E. Shuryak, Phys. Rev. Lett. **81**, 4816 (1998).
3. see, e.g., Proceedings of 14th International Conference on Ultrarelativistic Nucleus-Nucleus Collisions (Quark Matter 99), Torino, Italy, 10-15 May 1999, Nucl. Phys. **A661** (1999) 1c, and references therein.
4. O. Scavenius, A. Dumitru, E.S. Fraga, J.T. Lenaghan and A.D. Jackson, hep-ph/0009171.
5. L.D. Landau and E.M. Lifshitz, "Fluid Mechanics", Pergamon, New York, 1959.
6. B.D. Serot and J.D. Walecka, Adv. Nucl. Phys. **16** (1986) 1; D.H. Rischke, Y. Pürsün and J.A. Maruhn, Nucl. Phys. **A595** (1995) 383.

7. L.P. Csernai and J.I. Kapusta, Phys. Rev. **D46** (1992) 1379.
8. D.H. Rischke, Nucl. Phys. **A610** (1996) 88c.
9. H. Stöcker and W. Greiner, Phys. Rept. **137** (1986) 277; N.S. Amelin et al., Phys. Rev. Lett. **67** (1991) 1523.
10. P. Danielewicz and G. Odyniec, Phys. Lett. **B157** (1985) 146.
11. J. Brachmann, A. Dumitru, H. Stöcker and W. Greiner, Eur. Phys. J. **A8** (2000) 549.
12. L.P. Csernai and D. Röhrich, Phys. Lett. **B458** (1999) 454; J. Brachmann et al., Phys. Rev. **C61** (2000) 024909.
13. H. Liu *et al.* [E895 Collaboration], Phys. Rev. Lett. **84** (2000) 5488.
14. J.D. Gunton, M. San Miguel and P.S. Sahni, "The Dynamics of First-Order Phase Transitions", in: "Phase Transitions and Critical Phenomena", edited by C. Domb and J.L. Lebowitz, Academic Press, London, 1983, volume 8.